

## Secondary Atomization of Coal-Water Fuel Droplets Resulting from Exposure to Intense Radiant Heating Environments

Daniel J. Maloney and James F. Spann (ORAU)

U.S. DOE, Morgantown Energy Technology Center  
P.O. Box 880, Morgantown, WV 26505

### Introduction

The use of coal-water fuels (CWF) for direct firing in heat engines presents some challenges because conventional turbine combustors and diesel engines require short duration, intense combustion processes. It is generally understood that burning times required for efficient carbon utilization in these systems is a function of the fuel droplet size. For CWF droplets, the early stages of heating are critical. Under certain heating conditions, water is evaporated from a droplet leaving a relatively slow burning agglomerate of coal particles. Under other heating conditions, however, fuel droplets may boil explosively producing many small fragments having characteristically shorter combustion times. The behavior of CWF in a combustor depends on a number of factors including droplet size, the amount and size distribution of coal particle inclusions, and the primary mode and rate of droplet heating. A detailed knowledge of slurry droplet evaporation mechanisms is required, therefore, for accurate prediction of slurry droplet combustion times and for the design of CWF-fired heat engines.

The objective of this work is to determine the radiant energy flux conditions required to achieve explosive boiling of CWF droplets. Radiant heating is important because, when considering coal particle sizes typical of highly beneficiated micronized CWF (2 to 3 microns mean radius) proposed for use in heat engine applications, the black body radiation prevalent in combustion environments can penetrate into the droplet. The resulting internal heating of coal particles can result in superheating of the water within the droplet and thereby establish conditions necessary for explosive boiling.

Experimentally, conditions required to achieve explosive boiling were determined by electrostatically suspending and irradiating single CWF droplets with well characterized radiation pulses. Droplet behavior in these experiments was monitored using high-speed cinematography. The energy flux required for explosive boiling was determined at ambient temperature and pressure as a function of incident radiation intensity and CWF droplet size and composition. The results were then compared with theoretical predictions of the explosive boiling threshold for CWF droplets in high-temperature black body radiation fields. The primary question we wish to address is: do sufficient conditions exist, or can they be made to exist, to cause explosive boiling of CWF droplets ranging from 20 to 200 microns in diameter in realistic combustor configurations?

### Experimental

Single CWF droplets were isolated and held in an electrodynamic balance apparatus which was designed and fabricated based on the work of Davis and Ray (1). The balance, as illustrated in Figure 1, is a quadrupole trap consisting of two hyperboloidal endcap electrodes and a central ring electrode. When an AC voltage is applied between the ring and the two endcap electrodes the resulting field has a well defined null point at the geometric center of the balance. A charged droplet in the electric field is subject to a time averaged force directed toward the null point. The droplet is held at the null point by

applying a DC field across the endcap electrodes to counterbalance gravitational forces.

CWF droplets are delivered to the balance chamber from a CWF droplet generator developed specifically for use in these experiments. The basic device consists of a cylindrical piezoelectric transducer element with a capillary tube attached to one end and a fuel supply line attached to the other. The operating principle is the same as that used in ink-jet printers. Voltage pulses applied to the transducer cause sudden volume contractions which force fuel through the capillary orifice. The extruded fuel forms a monodisperse stream of droplets of uniform composition with the droplet size being determined by the capillary diameter and by the amplitude and duration of the voltage pulses. Details of the design and operating characteristics of the CWF droplet generator are provided elsewhere (2). Droplets are inductively charged by passing the droplet stream through an orifice in a charged plate prior to delivery into the electrodynamic balance chamber.

The droplet mass to charge ratio ( $m/q$ ) is directly proportional to the DC voltage required to bring the droplet to the null point. For CWF droplets the mass (and so  $m/q$ ) is continuously changing due to water evaporation and the balance voltage must be adjusted to hold the droplet at the null point during an experiment. To facilitate droplet position control and to provide accurate and precise measurements of changes in droplet size and mass, a microprocessor controlled, droplet imaging system (DIS) was developed. The DIS utilizes a Vidicon (video camera) detector to monitor droplet position and size. A microprocessor scans the vidicon every 17 ms and image processing techniques are employed to determine the droplet location and size. A control signal is then generated to maintain droplet position at the balance null point. Digital values corresponding to droplet cross-sectional area and balancing voltage (proportional to droplet mass) are generated at a rate of 60 Hz. The droplet size information is used to trigger the high-speed camera and to activate the pulsed radiation (laser) source. In addition, droplet diameter, mass and composition (percent coal by mass) are determined from the droplet size and balance control data. Figure 2 illustrates the capabilities of the DIS for droplet size and mass determination. The data shows the strong dependence of the droplet mass with changing droplet radius. Since droplet density increases as water evaporates from the CWF, the droplet mass dependence deviates slightly from the  $r^3$  relationship expected for a constant density droplet. The confidence interval (95 percent) for droplet size resolution with the DIS is  $\pm 3$  microns for droplets ranging in diameter from 50 to 200 microns. The confidence interval for mass resolution is  $\pm 50$  nanograms.

The CWF used in these experiments was a physically beneficiated (3 percent ash) micronized (3 micron mean particle radius) slurry having a composition of 62 percent coal by mass. During a typical experiment a water or dilute CWF (1 to 20 percent coal by mass) droplet was delivered to the balance chamber. The droplet size and weight were monitored by the DIS until a preselected size was attained. The high-speed movie camera was then activated and the laser was pulsed. A schematic of the experimental configuration is provided in Figure 3.

CWF droplets delivered to the balance chamber were on the order of 250 microns in diameter. Droplet size and composition were controlled by changing the initial coal composition in the droplet and by carefully monitoring the water evaporation. In this manner droplet sizes (50 to 200 microns in diameter) and compositions (50 to 70 percent coal by mass) of interest for combustion applications could be easily accessed.

## Results

Experiments were conducted using an eximer laser (wavelength 0.248 microns) to determine explosive boiling thresholds for water and CWF droplets at radiation pulse times of 10 nanoseconds. The test variables included droplet size and composition and radiation intensity. Single droplets of water and CWF (25 and 50 percent coal by mass) with radii of 25, 50, and 75 microns were irradiated from two sides (see Figure 3). The geometric cross section of the droplets then was twice  $\pi r^2$  and the incident radiation intensity was varied from  $2.5 \times 10^7$  W/cm<sup>2</sup> to  $5 \times 10^8$  W/cm<sup>2</sup> by defocussing the laser beam. At the most intense radiant heating conditions the beam cross section was larger than 300 microns so that in all cases the droplets were completely blanketed by the incident radiation.

The results of experiments performed on CWF droplets containing 50 percent coal by mass are presented in Figure 4. The results can best be described in the context of Figure 5. Over the range of conditions employed CWF droplet behavior varied from oscillatory distortions to violent fragmentation as the radiant intensity was increased. The onset of fragmentation occurred over a narrow range of intensities from about  $5 \times 10^7$  to  $1.5 \times 10^8$  W/cm<sup>2</sup>. Figure 5 shows high speed film records for 75 micron radius droplets containing 50 percent coal by mass. The framing rate was 5,000 frames per second. Figure 5A illustrates the oscillatory behavior observed for these droplets when irradiated at an intensity of  $2.5 \times 10^7$  W/cm<sup>2</sup>. At this radiant intensity no droplet fragmentation was observed. Lower radiation intensities resulted in no observable fragmentation or oscillation. When the radiant intensity was increased to  $5 \times 10^7$  W/cm<sup>2</sup> (Figure 5B) droplet fragmentation was observed. The first frame in sequence 5B shows the CWF droplet prior to initiation of the radiation pulse. The second frame of the sequence shows the droplet 0.2 ms later, after the laser pulse. The droplet appears to be a large prolated sphere suggesting the possible growth of vapor bubbles within the droplet. However, the time resolution available was not sufficient to conclusively show the existence of vapor bubbles. The third frame in the sequence shows the collapse of the prolated sphere and the formation of fuel "ligaments" attached to a central droplet core. This is followed by the breakup of the droplet to form three fragments. At this radiant heating intensity we consistently observed the formation of one or two small satellite fragments and a larger core droplet. After breakup, the fragments moved with a minimum velocity of 1 m/s. Figure 5C illustrates that as the radiant intensity was increased to  $1.2 \times 10^8$  W/cm<sup>2</sup> the fragmentation of the droplets was more violent resulting in the formation of many small fuel droplets having minimum velocities ranging from 0.5 to 2 m/s. At higher radiant intensities (Figure 5D), fragmentation was evident, however, droplet fragments had velocities in excess of 3 m/s and resolution of droplet fragments was poor.

Based on the different behavior evident in the high-speed film records modes of droplet behavior have been arbitrarily defined as: NF, no fragmentation of the droplets, F, fragmentation of the droplets to form a few relatively large droplet fragments, and EF, explosive fragmentation of the droplet to produce many small droplet fragments. Figure 4 summarizes the results of experiments using CWF droplets containing 50 percent coal by mass. The dashed line in the figure represents the theoretical predictions of Sitarski (3-5) for explosive boiling thresholds for CWF droplets exposed to high-temperature black body radiation. The theoretical predictions illustrated in Figure 4 have been modified to reflect the fact that the droplets were irradiated from two sides with a geometric cross section of  $2\pi r^2$ . Figure 4 illustrates that explosive boiling thresholds decreased as droplet size was reduced. Experiments performed on droplets with 25 percent coal by mass showed a similar trend with decreasing

droplet size. Within the error of the experiment there was no observable difference between the behavior of CWF droplets as the coal loading was increased from 25 to 50 percent coal by mass. The presence of coal in the droplet did play an important role, however. Pure water droplets showed no evidence of oscillation or fragmentation at radiation fluxes of  $5 \times 10^8$  W/cm<sup>2</sup> and below. This observation is consistent with the fact that pure water is essentially transparent to radiation at 0.248 micron wavelength.

### Discussion

The theory developed by Sitarski (4) assumes that electromagnetic radiation is absorbed uniformly within the droplet causing strong superheating of the liquid at the center of the droplet where thermodynamic conditions approach those on the spinodal line. The sudden burst of vapor bubbles produced at the spinodal temperature then leads to disruption of the droplet. The experimental observations are consistent with this physical description of the explosive boiling phenomena and the agreement between the experimentally determined thresholds for explosive fragmentation are in excellent agreement with the explosive boiling thresholds predicted by Sitarski.

Two alternative mechanisms for droplet breakup were also considered. They were the effect of radiation pressure and the potential for significant ionization and plasma formation. Calculations were performed to evaluate the radiation pressure associated with the laser pulse. The momentum imparted to the droplet due to the light pressure was found to be two orders of magnitude lower than the observed momentum (determined from the velocity of the fragments). Therefore, the contribution due to radiation pressure was insignificant. At radiation intensities similar to those employed in the present study, plasma formation has been observed for aerosol particles in air (6, 7). The accompanying laser breakdown depends on a number of factors including, the radiation wavelength, intensity and pulse time and the optical properties and size of the aerosol particles. Plasma formation and growth is usually accompanied by a characteristic flash of light followed by an acoustic pressure pulse (shock wave) as the plasma cloud expands at a rate of 2 to 3 km/s. Over the range of radiant heating conditions reported in Figure 4 there were no observations supporting the formation of a plasma cloud. At radiation intensities above  $10^9$  W/cm<sup>2</sup>, however, the characteristic signs of plasma formation were evident.

### Conclusion

Capabilities have been developed to determine radiant intensities required to achieve explosive boiling (secondary atomization) of CWF droplets of well defined size and composition. The system has been used to determine explosive boiling thresholds for CWF droplets at short duration high intensity radiant heating conditions. The experimental results are both qualitatively and quantitatively in good agreement with theoretical predictions for explosive boiling thresholds. Attention has now been directed toward applying these techniques to make measurements of explosive boiling thresholds at radiation wavelengths in the infrared region of the energy spectrum with millisecond heating times to address conditions which are representative of combustion applications.

### Acknowledgements

The efforts of G. E. Fasching and L. O. Lawson in the development of the DIS are gratefully acknowledged. Discussions with Dr. M. Sitarski have been stimulating and insightful and are gratefully appreciated. This work was funded out of the United States Department of Energy Advanced Research and Technology Development Program.

## References

1. Davis, E. J., and A. K. Ray, J. Colloid and Interface Science, 75, 566-576, 1980.
2. Maloney, D. J., L. A. McCarthy, W. F. Lawson, G. E. Fasching, and K. H. Casleton, "Laboratory Coal-Water Fuel Droplet Generator," Sixth International Symposium on Coal Slurry Combustion and Technology, Orlando, Florida, June 25 to 27, 1984.
3. Sitarski M., "Thresholds for Explosive Evaporation of Water and Coal-Water Mixture Fine Droplets Exposed to High-Temperature Black Body Radiation," Proceedings of Condensed Papers, International Symposium-Workshop on "Particulate and Multi-Phase Processes," 16th Annual Meeting of the Fine Particle Society, Miami Beach, Florida, April 22 to 26, 1985.
4. Sitarski, M., "Modification of an Analytical Model Which Predicts the Effect of Radiative Heating on Two-Phase Aerosols," presented at the AR&TD Direct Utilization Contractors Meeting, Morgantown, West Virginia, August 13 to 15, 1985.
5. Sitarski, M., Private Communication, October, 1985.
6. Danilychev, V. A., and V. D. Zvorykin, JSRLDU 5(6), 647-758, 1984.
7. Akhtyrchenko Y. V., L. A. Vasil'ev, Y. P. Vysotskii, and V. N. Soshnikov, JSRLDU, 5(2), 233-236, 1984.

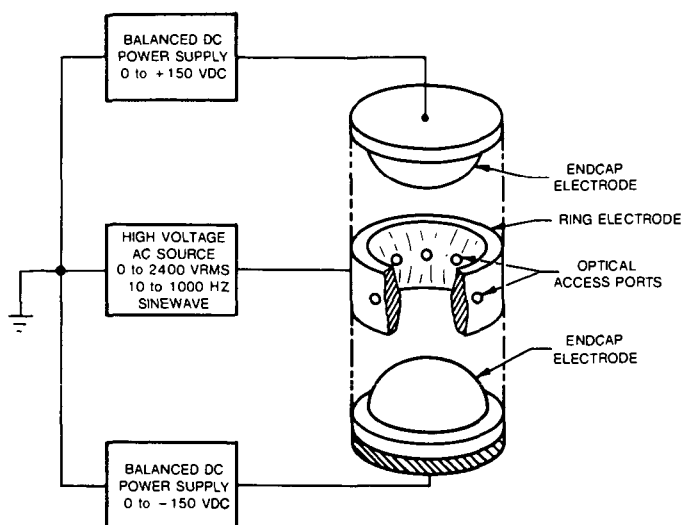


Figure 1. Electrodynamic Balance Apparatus

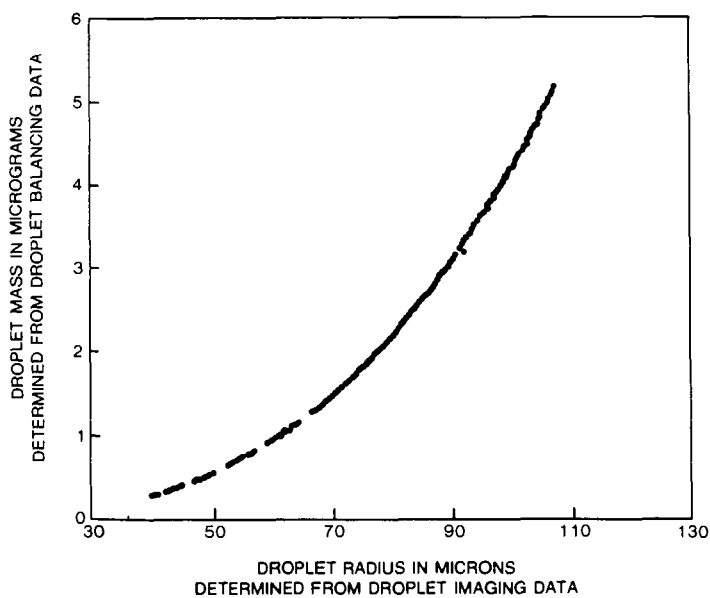


Figure 2. Droplet Mass and Size Resolution Capabilities for an Evaporating CWF Droplet

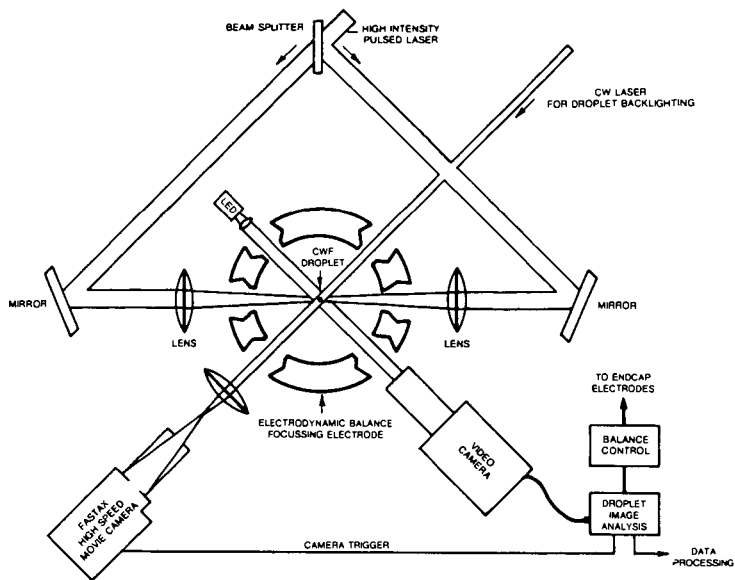


Figure 3. Experimental Configuration for Explosive Evaporation Studies

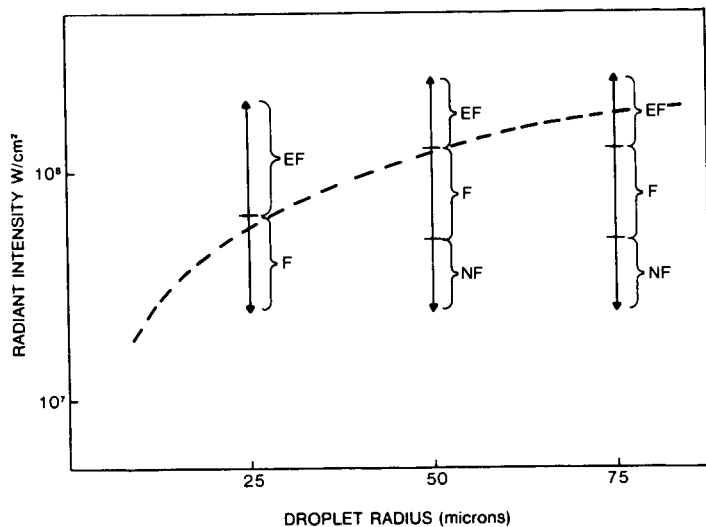


Figure 4. CWF Droplet Response as a Function of Radiant Heating Intensity at 10 ns Heating Time

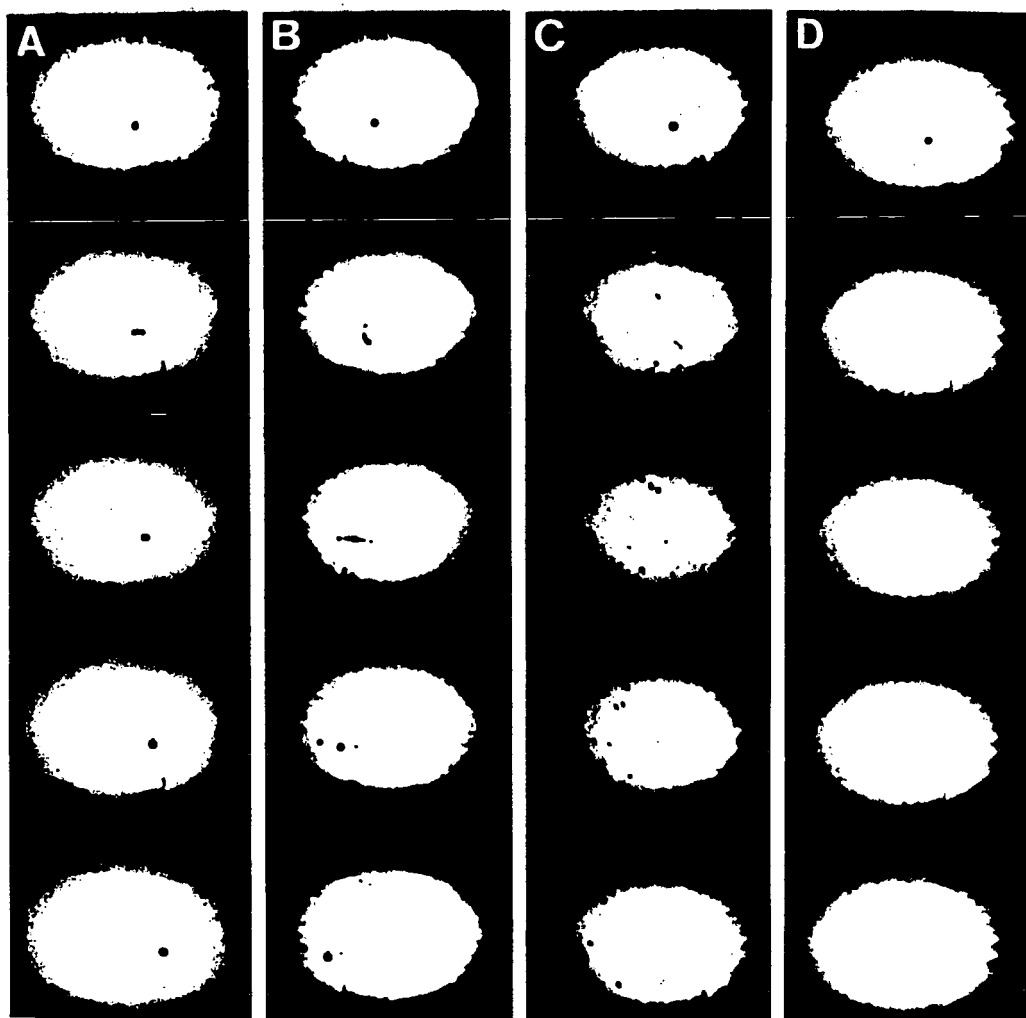


Figure 5. High-Speed Motion Picture Records of CWF Droplet Response to High-Intensity Radiant Heating. Radiant Intensity: A -  $2.5 \times 10^7$  W/cm<sup>2</sup>, B -  $5 \times 10^7$  W/cm<sup>2</sup>, C -  $1.2 \times 10^8$  W/cm<sup>2</sup>, D -  $2.5 \times 10^8$  W/cm<sup>2</sup>. Framing Rate of 5000 fps.